Polymer Journal (2019) 51:155–160
https://doi.org/10.1038/s41428-018-0133-8

ORIGINAL ARTICLE

Network structure evolution of a hexamethylenetetramine-cured phenolic resin

Atsushi Izumi[1] · Yasuyuki Shudo[1,2] · Mitsuhiro Shibayama[2]

Received: 19 July 2018 / Revised: 18 September 2018 / Accepted: 19 September 2018 / Published online: 22 October 2018

Abstract

The network structure evolution of a hexamethylenetetramine (HMTA)-cured novolac-type phenolic resin over a curing temperature range of 135–155 °C was investigated using ^{1}H-pulse nuclear magnetic resonance spectroscopy and small-angle and wide-angle X-ray scattering techniques. The aim was to elucidate the mechanism responsible for the apparent absence of inhomogeneity after curing at 175 °C, in which the inhomogeneity was first observed at the gel point below 130 °C. The HMTA-cured phenolic resin exhibited high-cross-link and low-cross-link density domains (denoted as HXD and LXD, respectively). The LXD was a minor structure having a cross-link fraction of 0.2, which was 5–6 nm in size and comprised a few meshes. As curing proceeded, intradomain reactions in the LXD occurred, and the electron density in the domain increased, decreasing the electron density difference between the HXD and LXD. This reduction in the electron density difference decreased the cross-link inhomogeneity in the phenolic resins in terms of electron density fluctuations. This structural evolution caused the apparent absence of inhomogeneity in the fully HMTA-cured phenolic resins.

Introduction

Since Baekeland invented phenolic resins as the first artificial plastics in 1907, they have been used as thermosetting resins in many industries over the past century. Cured phenolic resins have cross-linked network structures that comprise phenolic rings and methylenes, which can be typically obtained by curing novolac-type phenolic resin oligomers using hexamethylenetetramine (HMTA) as a curing agent [1].

Cured phenolic resins have been speculated to inevitably exhibit cross-link inhomogeneity that could strongly influence their mechanical properties [2, 3]. However, details of this cross-link inhomogeneity have not been fully elucidated because of the challenge of structural analysis of fully cured resins, which arises from their insolubility, infusibility, and noncrystallinity. Therefore, an experimental study of the inhomogeneity is still an important research topic to characterize the structure–property relation. This issue is not limited to phenolic resins but is common also an issue for other thermosetting resins [2–11].

We investigated the cross-link inhomogeneity in phenolic resins by using small-angle and wide-angle X-ray and neutron scattering and ^{1}H-pulse nuclear magnetic resonance (NMR) spectroscopy [12–15]. The scattering and NMR methods provide information about fluctuations in density and about the dynamics of the network structure, respectively [16–24]. These methods have been widely used to elucidate the inhomogeneity in cross-linked polymers, such as gels and rubbers. In addition, they are typically used in conjunction with a solvent-swelling technique to enhance the inhomogeneity on the basis of the local cross-link-density dependence of the swelling behavior. As one of our research achievements, we demonstrated that the solvent-swelling technique is applicable to phenolic resins near their gel points when the network structures are in the early stage of development [13–15]. In the previous study, the evolution of the network structure of HMTA-cured novolac-type phenolic resins at the initial stage of curing in the temperature range of 110–130 °C was investigated using these

✉ Atsushi Izumi
atsushi_i@sumibe.co.jp

✉ Mitsuhiro Shibayama
sibayama@issp.u-tokyo.ac.jp

[1] Corporate Engineering Center, Sumitomo Bakelite Co., Ltd., 2100 Takayanagi, Fujieda, Shizuoka 426-0041, Japan

[2] Neutron Science Laboratory, Institute for Solid State Physics, The University of Tokyo, 5-1-5 Kashiwanoha, Kashiwa, Chiba 277-8581, Japan

methods [15]. Here, the curing degree increases by increasing the curing temperature so that the structure evolution proceeds with the increase in temperature. The phenolic resin exhibited the cross-link inhomogeneity from the beginning of the curing. The inhomogeneity was observed as the presence of high-cross-link-density domains (HXD), low-cross-link-density domains (LXD), and the interface region among these domains. The dominant reactions over the investigated temperature range were intradomain reactions inside the HXD and LXD. There was no substantial change in the spatial location or size of these domains. The presence of the inhomogeneity after the gel point was confirmed by our theoretical analysis using a large-scale atomistic molecular dynamics (MD) simulation [25]. However, such cross-link inhomogeneity was not observed in HMTA-cured phenolic resins after curing at 175 °C through X-ray and neutron scattering analyses [12].

In the present study, to elucidate the disappearance mechanism of the HMTA-cured novolac-type phenolic resins' inhomogeneity that formed at the beginning of the curing process, the network structure evolution over the temperature range of 135–155 °C, which is well above the gel point as well as below the curing temperature of the typical novolac/HMTA curing system, was investigated by ^{1}H-pulse NMR and small- and wide-angle X-ray scattering (SAXS and WAXS, respectively) methods together with the solvent-swelling technique using methanol-d_4 (MeOD). A partly deuterated phenolic resin with a proton/deuterium (H/D) contrast between cross-links and other polymer segments was used to observe the dynamics of the cross-links via NMR analysis, where the polymer was prepared via curing of a deuterated novolac-type phenolic resin oligomer (NVD) with nondeuterated HMTA.

Experimental

Materials

NVD was prepared according to the method described in a previous literature [26]. HMTA and MeOD (99.8 atom% D) were purchased from Kishida Chemical Co., Ltd. (Japan) and Wako Pure Chemical Industries, Ltd. (now FUJIFILM Wako Pure Chemical Corp., Japan), respectively.

Curing reaction and sample preparation

Curing reactions of NVD with HMTA were performed using an NVD/HMTA weight ratio of 1/0.12. The NVD/HMTA mixture (5 g), which was melt-mixed at 120 °C for 30 min and then powdered, was heated from 135 to 155 °C stepwise in +5 °C increments under atmospheric pressure in a hot-air oven. The holding time was 30 min at each curing temperature. A 0.25-g sample collected at each set temperature was powdered and stirred in approximately 5 mL of MeOD at 40 °C for 3 days. Then, the resulting insoluble gels were washed with MeOD three times and collected as a fully MeOD-swollen phenolic resin.

^{1}H-pulse NMR spectroscopy

The ^{1}H-pulse NMR experiments were performed using an MQC23 benchtop NMR spectrometer (Oxford Instruments, UK) with a 10-mm-diameter probe operated at 23 MHz. Glass NMR tubes with a diameter of 10 mm and a wall thickness of 0.6 mm (JEOL RESONANCE Inc., Japan) were used as sample cells. The proton nuclear spin–spin relaxation decay was recorded at 40 °C using Carr–Purcell–Meiboom–Gill pulse sequences. The pulse width, pulse interval (τ), number of (180°−2τ)-loops, relaxation delay between subsequent scans, and number of scans were set to 2.0 μs, 25 μs, 4096, 3 s, and 512, respectively.

SAXS and WAXS

SAXS experiments over a q range from 0.03 to 4 nm^{-1} with an X-ray wavelength (λ) of 0.10 nm were performed at the second hutch of the BL03XU beamline at SPring-8, Hyogo, Japan. The details of the beamline were provided in the literature [27, 28]. Here, q represents the magnitude of the scattering vector given by $q = (4\pi/\lambda)$ sin $(2\theta/2)$, where 2θ denotes the scattering angle. A Pilatus3S 1M (DECTRIS Inc., Switzerland) was used as the X-ray detector. WAXS experiments over a q range from 1 to 35 nm^{-1} with $\lambda =$ 0.154 nm of a Cu Kα spectrum line were performed on a NANO-Viewer system (Rigaku Corp., Japan). A Pilatus 100K was used as the X-ray detector. For both experiments, quartz capillaries with a diameter of 2 mm and a wall thickness of 0.01 mm (Mark-tube, Hirgenberg gmbh, Germany) were used as sample cells. All measurements were performed at room temperature.

Results and discussion

Figure 1 shows the proton nuclear spin–spin relaxation decay profiles of the cross-links obtained in the fully MeOD-swollen state at 40 °C. The decay behavior was essentially the same irrespective of the curing temperature, i.e., irrespective of the curing progress. This observation suggests that the average local network structure that affected the dynamics of the cross-links was already determined at 135 °C, which supports our radial distribution function analysis of the methylenes after the gel point that was calculated using a united-atom-model MD simulation [29]. According to our previous NMR studies, the relaxation behavior of the entire polymer

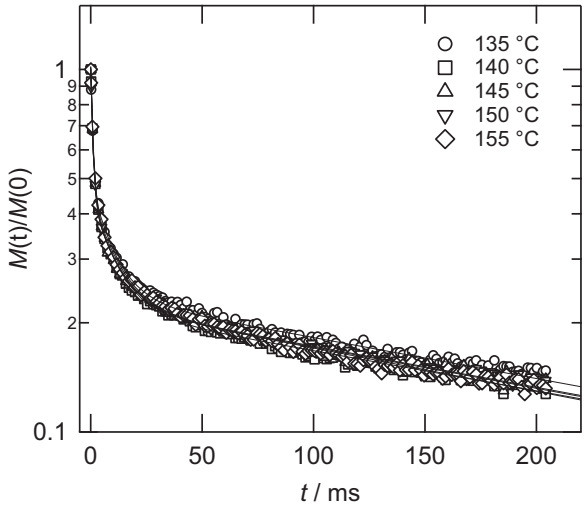

Fig. 1 Proton nuclear spin–spin relaxation decay profiles of the cross-links in the HMTA-cured phenolic resins. All the profiles were obtained in the MeOD-swollen state. Solid lines are fitting curves using Eq. 1

segments in the solvent-swollen state can be classified into three spin–spin relaxation modes due to the presence of the HXD, the interface region, and the LXD, and the relaxation time function follows a triple-exponential function [14, 15]. Assuming that the dynamics of the cross-links are affected not only by the dynamics of their local structure but also by that of their surrounding macroscopic structure, the spin–spin relaxation time function of the cross-links can be similarly expressed with the triple-exponential function given by

$$M(t)/M(0) = \phi_1 \exp(-t/T_{2,1}) + \phi_2 \exp(-t/T_{2,2}) + \phi_3 \exp(-t/T_{2,3}), \quad (1)$$

where t is the decay time; $M(t)$ denotes the magnetization intensity at t; and φ_i and $T_{2,i}$ ($i = 1$, 2, and 3) denote the molar fraction of protons on the cross-links and the time constant of the proton nuclear spin–spin relaxation in the i-th relaxation mode, respectively. Here, $\varphi_1 + \varphi_2 + \varphi_3 = 1$ and $T_{2,1} < T_{2,2} < T_{2,3}$. The relaxation becomes fast as the molecular mobility decreases. Therefore, the first and third relaxation modes are associated with the dynamics of cross-links in the HXD and the LXD, respectively, where the dynamics are highly constrained and less constrained, respectively. The second relaxation mode results from the dynamics of the cross-links in the interface region between the HXD and the LXD.

The curve fitting using Eq. 1 was successful, as shown in Fig. 1 with solid lines. The fitting parameters of $T_{2,i}$ and φ_i as a function of temperature are shown in Fig. 2a, b, respectively. As evident in Fig. 2a, three time constants were on the order of 10^0, 10^1, and 10^2 ms, which correspond to the HXD, the interface region, and the LXD, respectively. The three time constants for the entire polymer segment, including the cross-links, were 1, 40, and 600 ms at 130 °C, according to the previous study [15]. The good agreement of the set of the three time constants between the cross-links and entire polymer segments supports our conjecture that the dynamics of the cross-links were affected by the dynamics of their surrounding macroscopic structures. As Fig. 2b shows, each molar fraction of the cross-links in the three domains was essentially constant over the temperature range of 135–155 °C. The $\varphi_1/\varphi_2/\varphi_3$ ratio was approximately 0.6/0.2/0.2, which indicates that the cross-links with a fraction of 0.2 distributed in the LXD. These NMR results suggest that the curing of the phenolic resin proceeded without changing each type of domain or affecting the dynamics of the cross-links. In addition, these results suggest that the cross-link inhomogeneity in the HMTA-cured phenolic resins was determined at the beginning of the curing.

Figure 3a shows SAXS and WAXS profiles measured in the fully MeOD-swollen state. Here, the distinct peak around 10–20 nm^{-1} was caused by short-range correlations in amorphous structures of the resin and methanol molecules. The scattering intensity in the q range of 0.05–0.4 nm^{-1} decreased as curing proceeded. This behavior was due to the structural change of not only cross-links but the entire network structure and because the H/D-contrast in the polymer structure did not result in a substantial electron density contrast. Therefore, a previously proposed scattering function of solvent-swollen HMTA-cured phenolic resins can be applied to this system [15]. The function comprises five scattering terms that account for (i) the surface structure of solvent-swollen polymer particles, (ii) the solid-like frozen cross-link inhomogeneity, (iii) the liquid-like fluctuation of polymer segments, (iv) the short-range electron density fluctuation of polymer segments on the order of 10^{-1}–10^0 nm, and (v) the short-range correlation of MeOD molecules. The first term is known as Porod's law. The second and third terms are represented by the squared-Lorentzian equation ($I_{SL}(q)$) and the Ornstein–Zernike equation ($I_{OZ}(q)$), respectively, which are generally used together to express the cross-link inhomogeneity in a network structure. The fourth term is represented by a Gaussian function. The details of these scattering terms have been described in the literature [16–21]. The combined function is given by

$$I(q) = A \cdot q^{-4} + \frac{I_{SL}(0)}{\left(1 + \Xi^2 q^2\right)^2} + \frac{I_{OZ}(0)}{1 + \xi^2 q^2} + B \cdot \exp\left[-\frac{(q - q_0)^2}{2w^2}\right] + C \cdot I_{MeOD}(q), \quad (2)$$

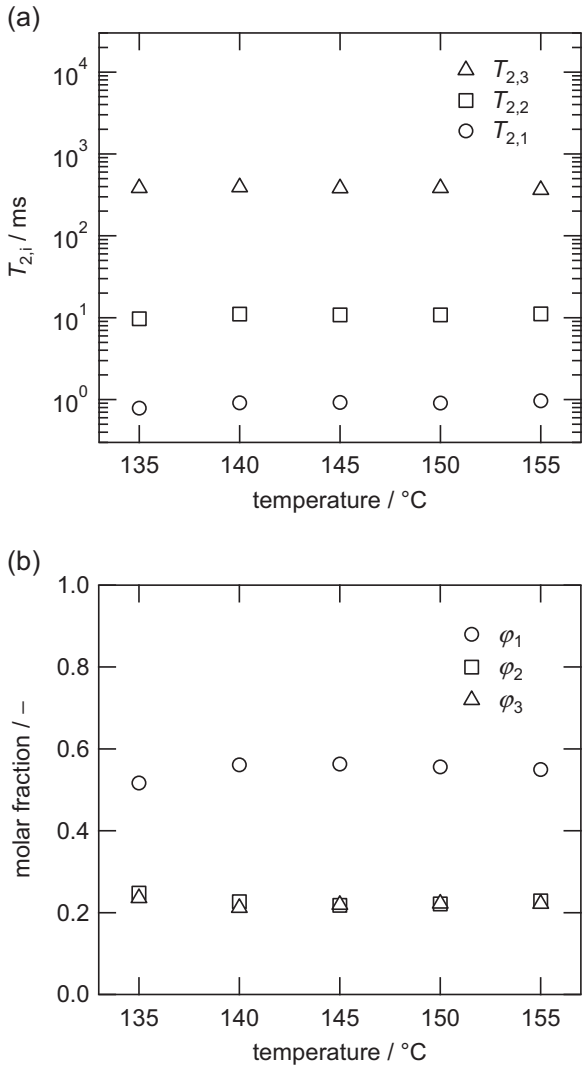

Fig. 2 Changes in **a** time constant representing the spin–spin relaxation and **b** molar fraction of the cross-links as a function of the curing temperature

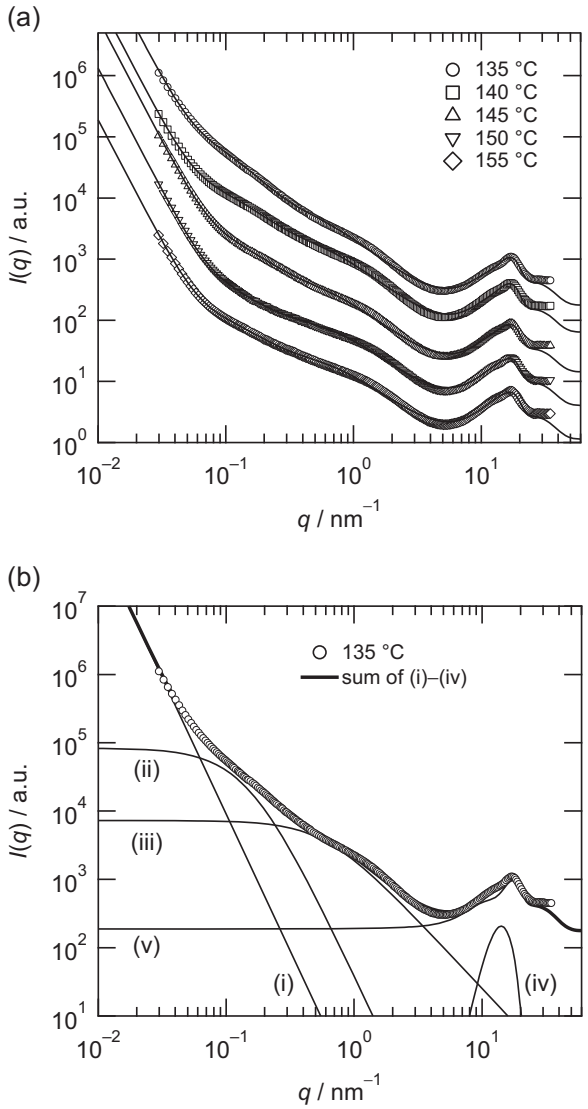

Fig. 3 **a** X-ray scattering profiles of the HMTA-cured phenolic resins. All profiles were obtained in the MeOD-swollen state. Solid lines are fitting curves using Eq. 2. **b** X-ray scattering profile of the resin cured at 135 °C (open circle) and the fitting curve using Eq. 2 (bold line). Curves (i)–(v) represent the first to five terms in Eq. 2

where $I(q)$ denotes the scattering intensity at q; Ξ denotes a correlation length that represents the characteristic size of the cross-link inhomogeneity; ξ denotes the correlation length of the concentration fluctuation, which behaves similar to a polymer chain in a semidilute regime; q_0 and w denote the peak position and peak width of the Gaussian function, respectively; $I_{\mathrm{MeOD}}(q)$ denotes the experimentally determined scattering function of MeOD; and A, B, and C are scaling factors. According to our previous study [15], when phenolic resins are well above the gel point, Ξ is associated with the average size of a minor domain in the system, i.e., the LXD, which was confirmed by the fraction φ_3 of 0.2. Additionally, ξ was associated with the average mesh size of the LXD. The interface region defined in the NMR analysis was considered part of the HXD in this scattering function.

As shown in Fig. 3a with solid lines, the curve fitting using Eq. 2 was successful. Figure 3a shows each contribution of the five terms on the right side in Eq. 2. Figure 4 shows the fitting parameters in the squared-Lorentzian and Ornstein–Zernike equations as a function of the curing temperature. As evident in these figures, $I_{\mathrm{SL}}(0)$ decreased with increasing temperature, whereas Ξ remained constant. This result suggests that the extent of cross-link inhomogeneity decreased without changing the sizes of the HXD or LXD. However, both the $I_{\mathrm{OZ}}(0)$ and ξ remained constant irrespective of the temperature, which suggests that no substantial structural change occurred within the LXD, such as a percolation reaction that would divide the mesh in the

domain. The Ξ value was 5–6 nm and was ~3–4 times as large as ξ, which indicates that each LXD comprised a few meshes. The absence of a substantial change in the structures over the investigated temperature range is consistent with the NMR results. However, the decrease in inhomogeneity without a substantial change in the structures appears to be contradictory. This can be explained by a reduction in the electron density difference ($\Delta\rho$) between the HXD and LXD because the scattering intensity is proportional to $(\Delta\rho)^2$. Intradomain reactions in the LXD without affecting the mesh size (i.e., chain propagation and branching reactions of dangling chains, which consume a space in the mesh) can decrease $I_{SL}(0)$, while other parameters remain constant. This explanation accounts for the NMR result that the dynamics of the cross-links in the LXD was not affected when the surrounding structure, i.e., the mesh size, was constant.

Summary

The evolution of the network structure of an HMTA-cured novolac-type phenolic resin was investigated over a curing temperature range of 135–155 °C. This temperature is well above the gel point and below the curing temperature of a typical novolac/HMTA curing system. The network structure exhibited the cross-link inhomogeneity with HXD and LXD from the beginning of the curing process. However, this inhomogeneity was not observed after curing at 175 °C in our previous study according to the X-ray and neutron scattering results. In this study, the inhomogeneity was observed because of the presence of the LXD as a minor structure, in which the molar fraction of the cross-links distributed in the domain was 0.2. The average size of the LXD was 5–6 nm, and the domain comprised a few meshes. As the curing proceeded, intradomain reactions in the LXD occurred over the curing temperature range from 135 to 155 °C. The intradomain reaction increased the electron density of the LXD, which decreased the electron density difference between the HXD and the LXD. This structural evolution resulted in an apparent absence of the cross-link inhomogeneity in the fully cured phenolic resins.

Acknowledgements The SAXS experiments were conducted at the second hutch of SPring-8 BL03XU (Frontier Softmaterial Beamline (FSBL)) constructed by the Consortium of Advanced Softmaterial Beamline with the proposal numbers 2017A7209 and 2017B7261. This work was supported by the Photon and Quantum Basic Research Coordinated Development Program by MEXT with the grant number 13004017. This study was conducted as part of the research activities of the Special Interest Group on Thermosetting Resins in the FSBL Consortium comprising the Asahi Kasei research group, the DENSO research group, and the Sumitomo Bakelite research group.

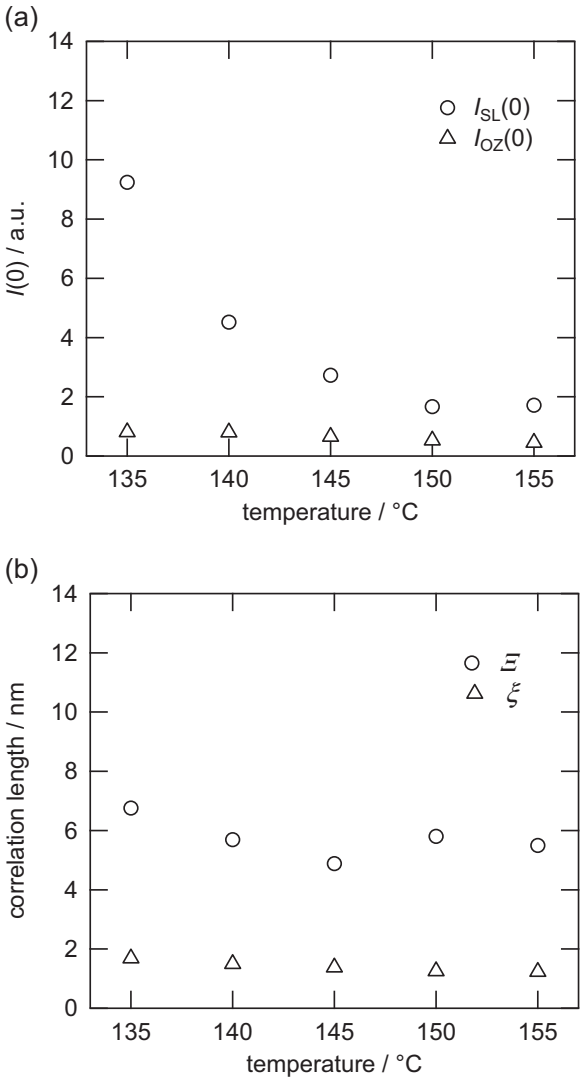

Fig. 4 Changes in **a** the zero-scattering intensity and **b** the correlation length as a function of the curing temperature

Compliance with ethical standards

Conflict of interest The authors declare that they have no conflict of interest.

References

1. Gardziella A, Pilato LA, Knop A. Phenolic resins: Chemistry, applications, standardization, safety and ecology. 2nd completely rev. edn. Berlin: Springer; 1999.
2. de Boer JH. The influence of van der Waals' forces and primary bonds on binding energy, strength and orientation, with special reference to some artificial resins. Trans Faraday Soc. 1936; 32:10–37.
3. Houwink R. The strength and modulus of elasticity of some amorphous materials, related to their internal structure. Trans Faraday Soc. 1936;32:122–31.

4. Pascault JP, Sautereau H, Verdu J, Williams RJJ. Thermosetting polymers. New York: Marcel Dekker; 2002.
5. Mijović J, Koutsky JA. Correlation between nodular morphology and fracture properties of cured epoxy-resins. Polymer. 1979; 20:1095–107.
6. Bai SJ. Crosslink distribution of epoxy networks studied by small-angle neutron-scattering. Polymer. 1985;26:1053–7.
7. Dušek K. Are cured thermoset resins inhomogeneous? Angew Makromol Chem. 1996;240:1–15.
8. Vanlandingham MR, Eduljee RF, Gillespie JW. Relationships between stoichiometry, microstructure and properties for amine-cured epoxies. J Appl Polym Sci. 1999;71:699–712.
9. Duchet J, Pascault JP. Do epoxy-amine networks become inhomogeneous at the nanometric scale? J Polym Sci, Part B: Polym Phys. 2003;41:2422–32.
10. Kishi H, Naitou T, Matsuda S, Murakami A, Muraji Y, Nakagawa Y. Mechanical properties and inhomogeneous nanostructures of dicyandiamide-cured epoxy resins. J Polym Sci, Part B: Polym Phys. 2007;45:1425–34.
11. Morsch S, Liu Y, Lyon SB, Gibbon SR. Insights into epoxy network nanostructural heterogeneity using AFM-IR. ACS Appl Mater Interfaces. 2016;8:959–66.
12. Izumi A, Nakao T, Iwase H, Shibayama M. Structural analysis of cured phenolic resins using complementary small-angle neutron and X-ray scattering and scanning electron microscopy. Soft Matter. 2012;8:8438–45.
13. Izumi A, Nakao T, Shibayama M. Gelation and cross-link inhomogeneity of phenolic resins studied by ^{13}C-NMR spectroscopy and small-angle X-ray scattering. Soft Matter. 2013; 9:4188–97.
14. Izumi A, Nakao T, Shibayama M. Gelation and cross-link inhomogeneity of phenolic resins studied by small- and wide-angle X-ray scattering and ^{1}H-pulse NMR spectroscopy. Polymer. 2015; 59:226–33.
15. Izumi A, Shudo Y, Nakao T, Shibayama M. Cross-link inhomogeneity in phenolic resins at the initial stage of curing studied by ^{1}H-pulse NMR spectroscopy and complementary SAXS/WAXS and SANS/WANS with a solvent-swelling technique. Polymer. 2016;103:152–62.
16. Roe RJ. Methods of X-ray and neutron scattering in polymer science. New York: Oxford University Press; 2000.
17. Bastide J, Candau SJ. Structure of gels as investigated by means of static scattering techniques. In: Cohen Addad JP, editor. Physical properties of polymeric gels. New York: John Wiley; 1996. pp. 143–308.
18. Wu WL, Shibayama M, Roy S, Kurokawa H, Coyne LD, Nomura S, et al. Physical gels of aqueous poly(vinyl alcohol) solutions: a small-angle neutron-scattering study. Macromolecules. 1990; 23:2245–51.
19. Shibayama M. Spatial inhomogeneity and dynamic fluctuations of polymer gels. Macromol Chem Phys. 1998;199:1–30.
20. Shibayama M. Small-angle neutron scattering on polymer gels: phase behavior, inhomogeneities and deformation mechanisms. Polym J. 2011;43:18–34.
21. Shibayama M. Structure-mechanical property relationship of tough hydrogels. Soft Matter. 2012;8:8030–8.
22. Cohen Addad JP (editor). NMR and statistical structures of gels. In: Physical properties of polymeric gels. New York: John Wiley; 1996. pp. 39–86.
23. Kimmich R, Fatkullin N. Polymer chain dynamics and NMR. Adv Polym Sci. 2004;170:1–113.
24. Asano A. NMR relaxation studies of elastomers. Annu Rep NMR Spectrosc. 2015;86:1–72.
25. Shudo Y, Izumi A, Hagita K, Nakao T, Shibayama M. Large-scale molecular dynamics simulation of crosslinked phenolic resins using pseudo-reaction model. Polymer. 2016;103:261–76.
26. Izumi A, Nakao T, Shibayama M. Synthesis and properties of a deuterated phenolic resin. J Polym Sci, Part A: Polym Chem. 2011;49:4941–7.
27. Masunaga H, Ogawa H, Takano T, Sasaki S, Goto S, Tanaka T, et al. Multipurpose soft-material SAXS/WAXS/GISAXS beamline at SPring-8. Polym J. 2011;43:471–7.
28. Takahara A, Takeda T, Kanaya T, Kido N, Sakurai K, Masunaga H, et al. Advanced soft material beamline consortium at SPring-8 (FSBL). Synchrotron Radiat News. 2014;27:19–23.
29. Izumi A, Shudo Y, Hagita K, Shibayama M. Molecular dynamics simulations of cross-linked phenolic resins using a united atom model. Macromol Theory Simul. 2018;27:1700103.